Copyright © 2014 American Scientific Publishers
All rights reserved
Printed in the United States of America

Journal of
Biomaterials and Tissue Engineering
Vol. 4, 973–980, 2014

Optimization of the Electrospinning Process for Core–Shell Fiber Preparation

Ying Li[1], Jian Liu[2], John R. de Bruyn[3], and Wankei Wan[1, 2, *]

[1] *Biomedical Engineering Graduate Program,* [2] *Department of Chemical and Biochemical Engineering,*
[3] *Department of Physics and Astronomy, The University of Western Ontario, London, Ontario N6A 5B9, Canada*

Electrospun core–shell fibers have gained increasing popularity in biomedical applications ranging from tissue regeneration to wound healing. Uniform fiber morphology and well-defined core–shell structure are critical for controlled delivery of bioactive molecules for these applications. In this work, core–shell fibers with rat tail collagen type I as the shell and a model protein, bovine serum albumin, as the core were prepared using coaxial electrospinning in both the horizontal and vertical configurations. High speed photography was used to observe the formation of the Taylor cone and fiber whipping motion during the fiber spinning process. Morphological considerations and core–shell structure of the fibers indicated that the vertical configuration is preferred for core–shell fiber preparation. The electrospun core–shell collagen fibers prepared using optimized experimental setup and parameters and crosslinked using genipin also demonstrated good cell compatibility properties.

Keywords: Tissue Engineering, Electrospinning, Electrospinning Setup, Core–Shell Fibers, Genipin Crosslinking.

Delivered by Publishing Technology to: Ying Li
IP: 129.100.226.75 On: Tue, 24 Nov 2015 16:24:27
Copyright: American Scientific Publishers

1. INTRODUCTION

Electrospinning is a simple and versatile technique to produce fibers with diameters down to a few nanometers and nonwoven architectures.[1] With the extremely high surface area to volume ratio, tunable porosity and ability to control the nanofiber composition to achieve the desired properties, electrospun nanofibers have found applications in many areas including filtration, protective material, electrical and optical applications, sensors, nanofiber reinforced composites, tissue engineering, drug delivery, etc.[2–12] More than 200 polymers and composite materials have been successfully electrospun into fibers.[2] A typical electrospinning set-up consists of a capillary, normally a needle attached to a syringe, through which the liquid to be electrospun is forced; a syringe pump to deliver the liquid consistently; a high voltage source; and a grounded collector.[13–15] During the electrospinning process, the fluid droplet delivered to the capillary tip is stretched under high electric field gradient, as it transverses the electric field, it solidifies into a fiber and deposited on a collecting electrode in the form of a random nonwoven mat.[13, 16, 17] The electrospinning process is highly dynamic and depends on the complex interplay between surface tension, electrical charges, and rheology, which has been the subject of many theoretical and experimental studies.[18–20] Experimental parameters that govern the electrospinning process can be divided into three categories: solution parameters such as viscosity, conductivity, molecular weight, and surface tension; process parameters such as applied electric field, tip to collector distance, and flow rate; and environmental parameters such as the humidity and temperature of the surroundings.[17, 21, 22] All these parameters play a significant role in determining the morphology and diameter of electrospun fibers.

Coaxial electrospinning, in which two polymer solutions are delivered independently through a coaxial needle, can produce fibers with a core–shell structure.[23] The coaxial electrospinning process is conceptually similar to that of single jet electrospinning. When a pendant droplet of the sheath solution elongates and stretches, the stresses generated in the sheath solution shear the core solution via "viscous dragging" and "contact friction".[24] This causes the core liquid to deform into a conical shape and a compound coaxial jet develops at the tip of the cone.[24] This process allows materials that cannot be electrospun in single jet electrospinning to be delivered in the core fluid and to form core–shell fibers.[25] Coaxial electrospinning has found wide applications, especially in the delivery and tissue engineering, in which bioactive agents such as DNA, gene and growth factors can be incorporated into the core for controlled and sustained release.[23, 24, 26, 27]

In general, the electrospinning setup can be either horizontal or vertical, as defined by the relative orientation of the electric field and the gravitational field.[28] Although

*Author to whom correspondence should be addressed.

RESEARCH ARTICLE

theoretically an infinite number of configurations are possible, in practice only the horizontal and the vertical configurations are in common use.[2, 24, 25, 28] In a horizontal electrospinning system, the electric force is perpendicular to gravity, while in the vertical system, the electric force is parallel to gravitational force. The vertical setup can be further sub-divided into shaft type, in which the ejecting capillary is above the collection target, and converse type, in which the ejecting capillary is below the collection target.[28] For vertical electrospinning by placing collector beneath the needle in shaft type configuration, gravitational force would enhance the spinning process, thus most studies are based on shaft type configuration and there have to date been few studies based on the converse electrospinning configuration.[28] It has been reported that gravitational force has an effect on the shape of the polymer droplet and the Taylor cone (TC), and therefore causes a difference in electrospinning parameters observed in horizontal and vertical systems.[29] However, among the more than 10000 publications on electrospinning to date, the attention paid to the effects of the electrospinning setup on the experimental parameters and fiber morphology and diameter is astonishingly low. There have been several studies on the effect of experimental configuration on the quality of electrospun solid fibers.[3, 28] Chakraborty et al. suggested that using the horizontal setup reduced the possibility of collecting imperfect fibers.[3] Yang et al. reported that configuration of the electrospinning setup affects fiber diameter and fiber diameter distribution.[28] To the best of our knowledge, there has been no reported study on the effect of electrospinning setup in the coaxial configuration on the formation and properties of the resulting core–shell fibers. Since uniform fiber morphology and well-defined core–shell structure are critical for controlled delivery of bioactive molecules to promote tissue regeneration, wound healing, and in many other applications, we report here a systematic study of the effect of horizontal and vertical electrospinning setups on the formation and properties of core–shell collagen fibers. The formation and shape of the TC and fiber whipping motion during the electrospinning process were observed using a high-speed video camera. Scanning electron microscopy (SEM) and transmission electron microscopy (TEM) were used to characterize the fiber morphology and core–shell structure. Fibrous scaffolds prepared using an optimized experimental setup and parameters were stabilized using genipin as a crosslinking agent. Cell compatibility was demonstrated using primary human skin fibroblasts.

2. MATERIALS AND METHODS

2.1. Materials

Type I collagen from rat tail was isolated, purified and lyophilized to powder form according to the protocol reported previously.[30] 1,1,1,3,3,3-hexafluoroisopropanol (HFIP), poly(ethylene glycol) (PEG) with molecular weight of 10 kDa were purchased from Sigma Aldrich (ON, Canada). Albumin from Bovine Serum (BSA), Alexa Fluoro® 594 conjugate, Alexa 488 Phalloidin SelectFX Nuclear Labelling Kit, and Prolong Gold Antifade Reagent were purchased from Invitrogen Canada Inc. Genipin crosslinking reagent was bought from Challenge Bioproduct Co. (Taiwan). Anhydrous ethyl alcohol was obtained from Commercial Alcohols (Canada) and glacial acetic acid was purchased from Caledon Labs (Canada). All reagents were used as received without further purification.

2.2. Preparation of Collagen/PEG-BSA Fibrous Scaffolds Using Coaxial Electrospinning

The shell solution was prepared by dissolving 84.2 mg collagen in 1 mL HFIP at a concentration of 5 wt%. The core solution was obtained by first dissolving PEG into 80% ethanol at a concentration of 200 mg/ml. BSA-Alexa Fluor® 594 was then added to the PEG-ethanol solution at a concentration of 100 μg/ml. The container was then wrapped with aluminum foil and the solution stored at 4 °C to preserve fluorescence.

Both the horizontal and vertical electrospinning processes were carried out at room temperature in a custom-built environmental control box, which was observed with a high speed camera with frame rate up to 2000 frames/second (Redlake MotionScope M, AOS Q-PRI and Olympus I-speed 3). A dual-syringe pump (Harvard Apparatus) was used to deliver the core and shell solutions independently to a custom-made stainless steel coaxial needle. The high electric field gradient between the needle and the collector was generated by a high-voltage DC power supply (Glassman High Voltage Inc.). Temperature and relative humidity were monitored with a Temperature/humidity monitor (Omega Engineering Inc). The experimental parameters explored were voltage (V), needle-to-collector distance (D), core solution flow rate (CFR), shell solution flow rate (SFR), and relative humidity (RH).

2.3. Morphological Characterization of the Electrospun Core–Shell Nanofibers

Fiber morphology was observed using a high resolution scanning electron microscope (Hitachi 3400S and LEO1530). ImageJ software (NIH, Bethesda, MD, USA) was used to measure the fiber diameters. Four SEM images were acquired at different locations for each sample and 30 fibers were randomly selected from each image and their diameters measured. Thus, the total fiber diameters measured for each sample were 120 fibers. The core–shell structure was observed using a Philips CM 10 TEM for both the side view and cross-sectional view. To obtain the cross-sectional view, the electrospun fibers were embedded in Spurr's Low Viscosity embedding mixture, cured at 60 °C for 48 hours and microtomed to a thickness of approximately 70 nm. TEM grids were stained with uranyl acetate before imaging.

Delivered by Publishing Technology
to: [illegible] Tue, 24 Nov 2015 [illegible]
Copyright: American Scientific Publishers

2.4. Genipin Crosslinking

The as-spun collagen fibers are unstable in aqueous environments. Therefore, crosslinking is essential to stabilize these fibers before cell seeding. Based on previous work on stabilization of solid collagen fibers,[31] genipin, a natural crosslinking agent which is far less cytotoxic than the commonly used glutaraldehyde, was used to crosslink the core–shell collagen fibers. Specifically, the crosslinking solution was prepared by adding genipin into a 3% solution of water in ethanol to reach a genipin concentration of 0.03 M (~11.3 mg of genipin per mg of collagen). The as-spun fibrous scaffolds were then immersed into the crosslinking solution for 5 days at 37 °C.

2.5. Cell Seeding, Staining and Imaging

Primary human skin fibroblasts were acquired from the palmar hand fascia of patients that underwent carpal tunnel release surgery as reported previously.[31] All subjects provided written informed consent under institutional review board approval and specimens were collected with the approval of the University of Western Ontario Research Ethics Board for Health Sciences Research involving Human Subjects (HSREB protocol No. 0822E). This conforms to the Code of Ethics of the World Medical Association (Declaration of Helsinki) for experiments involving humans. All fibroblasts cultures were used up to a maximum of 7 passages to ensure an *in vivo*-like morphology and response to their environment.

Delivered by Publishing Technology to: Yale Li
IP: 129.100.226.75 On: Tue, 24 Nov 2015 16:24:37
Copyright: American Scientific Publishers

To demonstrate the biocompatibility of the crosslinked collagen nanofibers, fibrous scaffolds were sterilized in ethanol for 30 minutes and primary human skin fibroblasts were seeded on these scaffolds to a concentration of 1.2×10^5 cells/well. After being cultured at 37 °C for 72 hours, the growth media was removed and the samples were rinsed with PBS on a shaker for five minutes. 1 ml of 4% paraformaldehyde was added to each well and the samples were incubated for 10 minutes to fix the cells. Alexa 488 phalloidin and DAPI were used to stain the actin filaments and cell nuclei, respectively. A Carl Zeiss laser scanning confocal microscope (LSM-410) equipped with an argon ion and a helium-neon laser was used to image the cell structure as well as detect the auto-fluorescence of collagen to characterize the fiber structure.

3. RESULTS AND DISCUSSION

3.1. Optimization of the Coaxial Electrospinning Conditions

The success of the electrospinning process depends on the formation of a stable TC at the tip of the needle. To ensure a continuous flow of the core material in the coaxial electrospinning process, a steady state compound TC needs to be formed. However, it was observed that the TC was distorted due to the gravitational force in the horizontal electrospinning configuration (Figs. 1(a) and (b)).

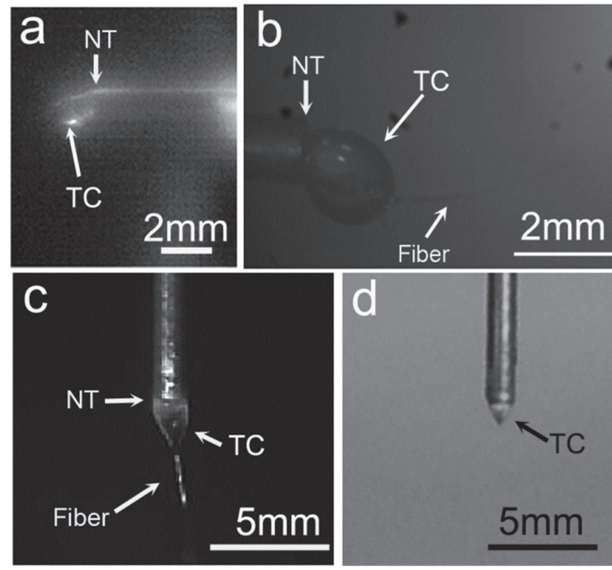

Fig. 1. Distorted Taylor cone (TC) on needle tip (NT) in horizontal electrospinning due to gravitational force, (a) before and (b) after fiber formation at the tip; stable compound TC formed at the NT in vertical coaxial electrospinning, (c) after and (d) before fiber formation.

This can be contrasted with the TC formed in the vertical setup, in which the gravitational force acts along the fiber-drawing direction and the TC always forms without distortion (Figs. 1(c) and (d)). Distortion of the TC can change with timing of the electrospinning process, which may result in unstable spinning due to extensive solution retention at the tip of the needle and possible solution mixing. It has been reported that the orientation of the experimental setup and the effect of gravity on the shape of the TC affects the electrospinning parameters required to achieve non-beaded fiber morphology.[29] Since fibers initiate from the surface of the TC, distortion of the TC may not affect the structure of solid fibers. In coaxial electrospinning, however, the stability of the compound TC is crucial to forming the core–shell structure, and distortion of the cone could prevent the formation of a uniform core–shell structure.

The effect of electrospinning parameters on fiber morphology and fiber diameter had been extensively studied for solid fibers.[17,21,22,29,32] Following a similar approach, the effect electrospinning parameters including voltage, needle-to-collector distance, solution flow rate, and relative humidity for core–shell collagen fiber formation have been studied in both the horizontal and vertical spinning configurations.

The optimal voltage range to produce bead free core–shell collagen-PEG fibers were determined to be 19–24 kV and 22–23 kV for horizontal and vertical coaxial electrospinning. The voltage range over which no beading was observed in the vertical configuration was narrower than in the horizontal configuration. This difference can be attributed to two factors. First, the curvature of the droplet

RESEARCH ARTICLE

formed at the tip of the needle may change with the distortion caused by gravitational force in horizontal electrospinning, and lead to a broader spinning voltage range. Also, in the horizontal electrospinning experiments, since the collector electrode is not beneath the spinneret, any spinning fluid droplets/beads formed due to gravity would not be deposited as beads among the fibers formed. In an electrostatically driven jet, the solution jet emission mode could be dominated by "spindle mode" or "cone-jet mode." In the "spindle mode," which is the transition mode from electrospraying to electrospinning,[33,34] solution jet and droplets spray out simultaneously. In horizontal coaxial electrospinning, these droplets may be deposited at locations other than the collecting electrode due to the influence of the gravitational force, while a portion of the fibers can still be carried to the collector by the electrostatic force and fiber whipping motion. On the other hand, in vertical coaxial electrospinning, any droplets will be collected on the substrate directly below the spinneret because both the electrostatic and gravitational forces act in the same direction. Only when the "cone-jet mode" dominates and no droplets are formed during the process can "perfect" fibers be collected in vertical electrospinning. Therefore, collecting smooth non-beaded fibers in vertical coaxial electrospinning requires a more restricted voltage range than in horizontal electrospinning. This result is in agreement with Chakraborty et al.,[3] who showed that horizontal electrospinning can eliminate the collection of imperfect products.

Delivered by Publishing Technology to: Ying Li
IP: 129.100.226.75 On: Tue, 24 Nov 2015 16:24:27
Copyright: American Scientific Publishers

The tip-to-collector distance was varied over the range of 5–8 cm. This distance determines the flight time of the fiber in the whipping process. A longer distance extends the flight time of the fibers and the greater stretch of the polymeric jet would result in thinner fibers. Therefore, a smaller fiber diameter is expected at increase tip-to-collector distance. As we are aiming to make fibers with small diameter, the tip-to-collector distance was increased. However, the increase in tip-to-collector distance has to be compensated for by a voltage increase to ensure to formation of stable TC, we found that at the optimal voltage we determined, the optimal distances that produced good morphology and fiber size were 7 and 6.5 cm for horizontal and vertical electrospinning respectively.

In previous preliminary work in our laboratory, we have determined that for the collagen-PEG core–shell system, the use of core and shell flow rate combination of 0.05 ml/hr–0.2 ml/hr, and 0.1 ml/hr–0.6 ml/hr resulted in the formation of core–shell fibers.[35] Using these data as the starting point, we determined that a core–shell flow rate combination of 0.06 ml/hr and 0.18 ml/hr resulted in the production of good quality core–shell collagen fibers. Higher core–shell flow rates with the same core–shell flow rate ratio produced fibers with beads-on-string morphology. Further change in flow rate ratio resulted in solution dripping, electrospraying of collagen beads or ribbon-like fibers. The 1:3 ratio of core–shell solution flow rate is consistent with the rates reported in the literature for Poly(caprolactone)/Poly(ethylene glycol) (PCL/PEG) core–shell fibers.[3,36] The effects of relative humidity are strongly coupled to other environmental parameters and operating conditions, so the coupled effects cannot be directly identified.[21] Depending on the hydrophilic-hydrophobic properties of the polymer and the solvent used, humidity can have a significant effect on the spinnability of the polymer solution and the quality of the resulting fibers. For hydrophilic polymers such as (PEG), to ensure the solvent in the whipping jet is fully evaporated during the flight time between the needle and the collector, not only a high vapor pressure for the solution is needed, the ambient humidity also must be relatively low.[37] We determined that good quality core–shell collagen fibers can only be formed at relative humidity ~30%.

Overall, we determined that for optimum fiber preparation, the experimental parameters that yielded core–shell collagen fibers with no beads in the horizontal configuration were $D = 7$ cm, CFR = 0.06 ml/hr, SFR = 0.18 ml/hr and $V = 19$–24 kV, while in the vertical configuration, these parameters were $D = 6.5$ cm, CFR = 0.06 ml/hr, SFR = 0.18 ml/hr and $V = 22$–23 kV. The relative humidity would be 30%.

3.2. Fiber Morphology and Core–Shell Fiber Structure

Figures 2(a) and (b) show SEM images of as-spun core–shell collagen fibers fabricated using the horizontal and vertical electrospinning setups, respectively. Most of these fibers have cylindrical morphology with diameters ranging from under 100 nm to less than 1000 nm. Figures 2(c) and (d) show the measured diameters of the horizontally and vertically electrospun core–shell fibers, respectively, fitted to a normal distribution function. At the same electrospinning voltage of 22 kV, the average diameters for horizontally and vertically electrospun core–shell fibers are 510 ± 140 and 310 ± 100 nm, respectively. The vertically electrospun core–shell fibers have a smaller average diameter and can be better fitted with a normal distribution function, which can be attributed to the narrower voltage range that is required to achieve non-beading electrospinning compared to the horizontally electrospun core–shell fibers.

The ideal core–shell fiber should have a uniform cylindrical morphology. In the bright field TEM images, the normal core–shell collagen/PEG-BSA fibers with cylindrical morphology have a lighter shell and darker core, as seen in Figures 3(a) and (b), which were taken from samples prepared using horizontal and vertical configurations, respectively. However, fibers with reversed contrast, i.e., darker shell and lighter core (Figs. 3(c) and (d)), were also observed in the samples prepared using similar experimental conditions. These fibers collapsed after the solvent evaporated and resulted in a ribbon or band-like shape as seen in the SEM image (Figs. 3(g) and (h)).

RESEARCH ARTICLE

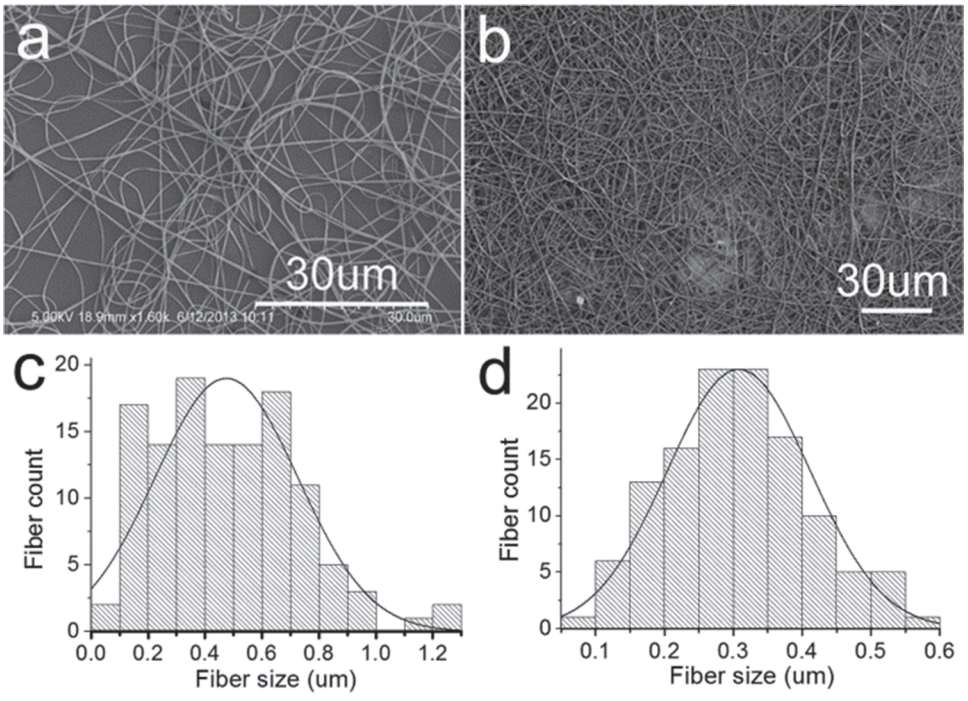

Fig. 2. No-beading core–shell fibers produced with (a) horizontal coaxial electrospinning, and (b) vertical coaxial electrospinning; histogram of core–shell fibers electrospun at 22 kV fitted with normal function, (c) horizontal spinning, average fiber diameter 509 ± 137 nm, and (d) vertical spinning, average fiber diameter 307 ± 96 nm.

In the fibers fabricated with both horizontal and vertical configurations, solid fibers were also observed (Figs. 3(e) and (f)). Theoretically, it is possible to obtain three different kinds of fiber structure in coaxial electrospinning as shown in Figure 4(a): well-defined core–shell structures which would be the ideal outcome; solid fibers formed by either the core or shell material; and composite fibers resulting from a mixture of the core and shell solutions. Both solid fibers made of the core or shell material and composite fibers made of a mixture of core and shell materials appear the same in the bright field TEM images if the fibers have a cylindrical morphology. Therefore, the solid fibers observed in horizontal coaxial electrospinning can be made of just the core or shell material, or a mixture of the core and shell materials. The reversed contrast seen in Figures 3(c) and (d) could be attributed to fibers with dog-bone shaped cross-section (Fig. 4(b)), which would yield a darker shell and lighter core in a bright field TEM image as more electrons can pass through the middle region of the band-shaped fibers than the electrons that can pass through edge region.

In order to further clarify the core–shell structure, cross-sectional TEM images were acquired from the microtomed core–shell nanofibers. In the cross-sectional images of collagen/PEG-BSA core–shell fibers, the core is brighter and the shell is darker. The image contrast comes from the different electron-scattering cross-sections of the core and shell materials. Figures 5(a) and (b) were taken from vertically electrospun samples and show a clear contrast between the core and shell, indicating a well-defined core–shell structure. However, in the samples prepared using horizontal electrospinning, the core–shell structure is less well-defined. The boundary between the core and shell is less clear (Fig. 5(c)) and in some fibers a mixture of core and shell materials was observed (Fig. 5(d)).

The uniformly distributed fiber diameter and well-defined core–shell structure obtained using the vertical configuration indicates that it is preferred over the horizontal configuration in coaxial electrospinning. This is consistent with the observed TC formed in the electrospinning processes in the two electrospinning configurations. It should be noted that the core and shell solutions used in this work are miscible. In the horizontal electrospinning configuration, the distorted TC (Figs. 1(a) and (b)) may lead to solution retention and mixing at the tip of the needle, which could lead to fibers with less well-defined core–shell structure. On the other hand, a steady state compound TC can be preserved during the vertical electrospinning process and mixing between the core and shell solutions can only occur by their mutual diffusion. It is estimated that the characteristic time for diffusive spreading of a sharp boundary between two identical polymers is approximately 10 times larger than the characteristic time of the bending instability in the electrospinning process.[25] Therefore the sharp boundary should survive in the coaxial electrospinning process even when miscible solutions are used, which is in agreement with the current observation in the vertical electrospinning configuration.

Copyright American Scientific Publishers

RESEARCH ARTICLE

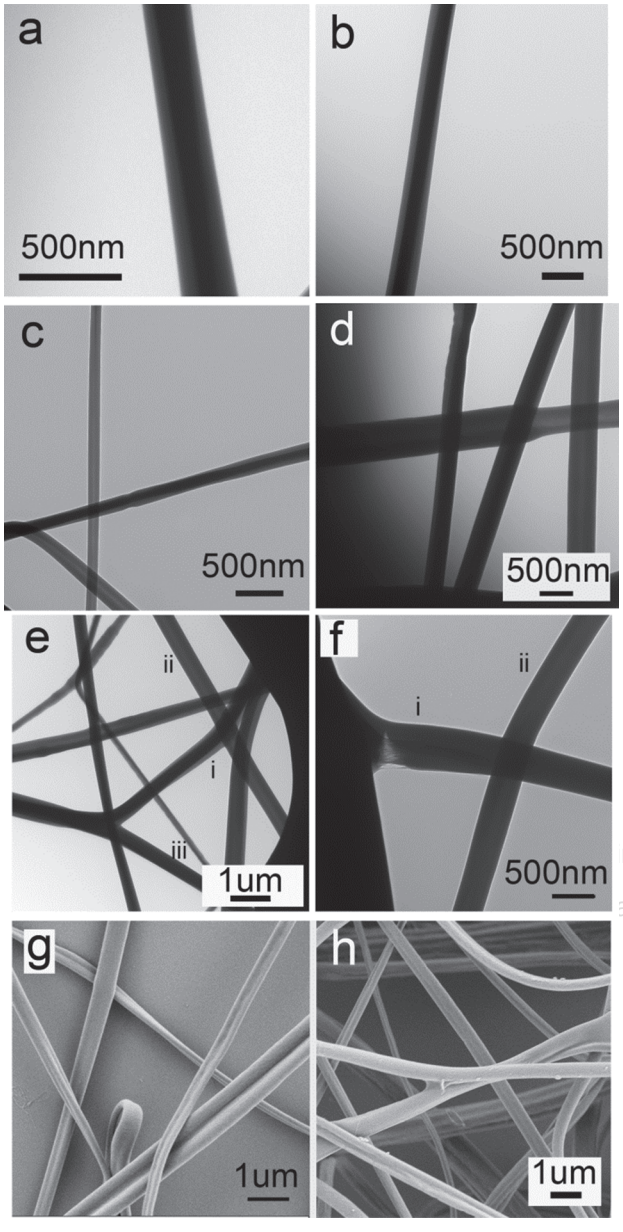

Fig. 3. TEM images of electrospun fibers, fibers showing core–shell structure from (a) horizontal spinning, (b) vertical spinning; fibers showing reverse contrast from (c) horizontal spinning, (d) vertical spinning; (e) existence of core–shell structure (region i), reverse contrast (region ii) and solid fibers (region iii) in horizontal spinning; (f) existence of core–shell structure (region i) and solid fibers (region ii) in vertical spinning; SEM images of collapsed fibers in (g) horizontal spinning and (h) vertical spinning.

3.3. Stabilization of Core–Shell Collagen Nanofibers Using Genipin Solution

The as-spun collagen nanofibers are unstable in aqueous environment. They readily disintegrate when in contact with water. Figures 6(a) and (b) show SEM images of as-spun collagen core–shell nanofibrous mats before and after being immersed in water for 5 seconds, respectively. The fiber morphology of the as-spun collagen immediately disappears on contact with water. After crosslinking

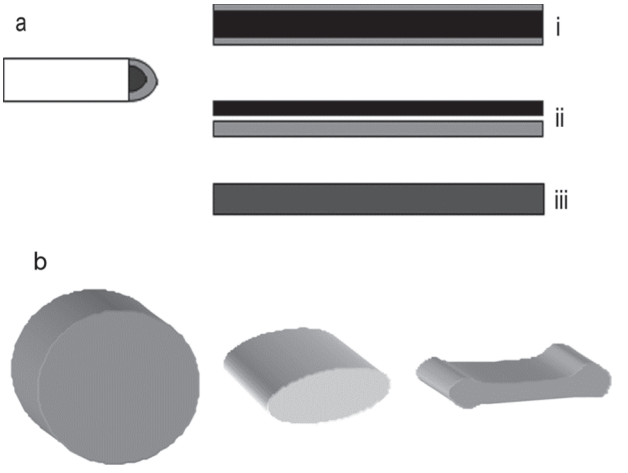

Fig. 4. (a) Three possible types of resultant fiber structure: (i) core–shell structure, (ii) separate core fibers and shell fibers, and (iii) composite fibers from blended mixture, (b) fiber collapsed resulting in non-cylindrical morphology and reversed contrast.

in genipin solution for 5 days, the fiber morphology is preserved (Fig. 6(c)). The average fiber diameter increased from 310 ± 100 nm to 720 ± 270 nm, indicating fiber swelling during the crosslinking reaction. The stability of the crosslinked samples was tested by placing them in water for 7 days. The SEM image (Fig. 6(d)) shows that these fibers survived after the test. However, the average size of the fibers decreased to 250 ± 140 nm, which can be attributed to collagen degradation over time. These results are consistent with our previous observation on genipin-crosslinked solid collagen fiber.[31] Since the degree

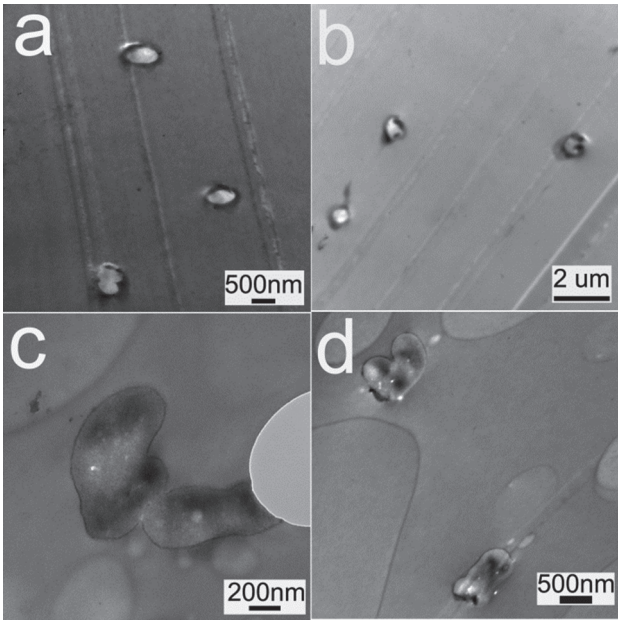

Fig. 5. Cross-sectional TEM images, (a) and (b) showing well-defined core–shell structure from vertical spinning; (c) showing non-uniform distribution of cross-section from horizontal spinning with dark shell and lighter core; (d) showing non-uniform distribution of cross-section from horizontal spinning with no distinctive core–shell boundary.

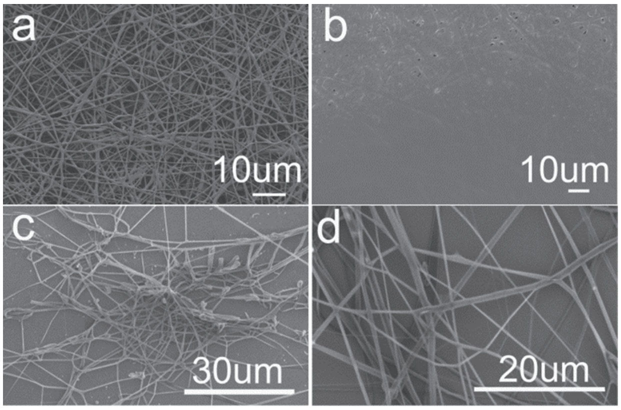

Fig. 6. SEM images of core–shell fibers from vertical spinning, (a) as-spun fibers, (b) immersed in water for 5 seconds, (c) after genipin crosslink, and (d) genipin crosslinked core–shell fibers after immersed in water for 7 days.

of crosslinking of solid electrospun collagen nanofibers can be tuned by adjusting the crosslinking conditions, it is expected that the crosslinking of core–shell collagen fibers can also be similarly controlled. The crosslinking of collagen fibers in a genipin solution starts from the surface of the fiber where the collagen is in contact with the crosslinking solution. The crosslinking is a self-limiting reaction as genipin has to diffuse through the crosslinked surface barrier. It is therefore possible to adjust the reagent concentration and reaction time to limit crosslinking to the collagen shell and leave the bioactive molecules in the core intact. This is very important in both tissue engineering and controlled release applications, as the activity of bioactive molecules has to be preserved. In the case of scaffolds for tissue regeneration which provide temporary support for cell growth, cell adhesion, proliferation, and extracellular matrix deposition, they should degrade at a rate commensurate with the rate at which tissue is regenerated. With the possibility of controlling crosslinking of the fibers, the fiber properties can also be tailored for optimal mechanical properties for cellular activities for the neo tissue regeneration process.

Delivered by Publishing Technology to: Ying Li
IP: 139.100.226.75 On: Tue, 24 Nov 2015 16:24:27
Copyright: American Scientific Publishers

3.4. Cell Seeding on Crosslinked Core–Shell Collagen Nanofibers

To test the cell compatibility of the crosslinked collagen core–shell nanofibrous scaffolds, primary human skin fibroblasts were seeded on the genipin crosslinked core–shell collagen scaffolds, cultured for 72 hours and imaged with laser scanning confocal microscopy (Fig. 7). Figure 7(a) shows the nucleus of these cells stained with DAPI. Figure 7(b) shows the filamentous actin cytoskeleton stained with phalloidin 488, and Figure 7(c) represents genipin crosslinked core–shell collagen fibers fluorescent in red. Figure 7(d) is an overlay of Figures 7(a)–(c). By using different excitation and emission wavelengths, the scaffold morphology and cell morphology can be clearly distinguished. Both the scaffold supported fibroblast attachment and the fibrous morphology of the crosslinked nanofibers were maintained over the cell growth period. The fibroblasts populated across the scaffold surface, which is an indication of good cell adhesion and biocompatibility of the scaffold. However, encapsulation of BSA does not affect cell behavior. To stimulate cell migration, growth factors should be incorporated. In the future, appropriate growth factors will be incorporated in the core–shell fibers. The release of these bioactive molecules in simulated body fluid to guide and signal cells for migration, adhesion and differentiation will be studied to demonstrate the usefulness of the core–shell collagen fiber system in tissue regeneration.

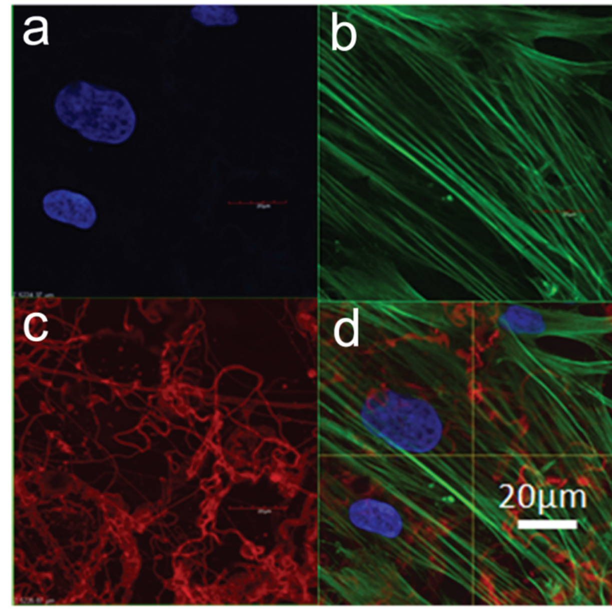

Fig. 7. Fluorescence images of primary human fibroblasts cultured on crosslinked BSA-PEG/collagen core–shell fibers (3D) showing (a) cell nucleus, (b) actin filament, (c) genipin crosslinked core–shell collagen fibers, and (d) overlay of (a)–(c).

4. CONCLUSION

The effect of coaxial electrospinning experimental setup configurations on the preparation and quality of core–shell collagen fiber was studied. It was shown that the fibers fabricated with vertical electrospinning have a better-defined core–shell structure, a smaller average fiber diameter and a narrower fiber diameter distribution than the fibers prepared with horizontal electrospinning. Therefore, the vertical configuration is preferred in the preparation of core–shell fibers with coaxial electrospinning. A natural crosslinking reagent, genipin, was effective in stabilizing the as-spun core–shell collagen fibers in aqueous environment. Cell culture studies with human skin fibroblasts demonstrated that the crosslinked core–shell collagen fibrous scaffold has good cell compatibility.

Acknowledgments: The authors would like to express their great appreciation to Dr. David B. O'Gorman

RESEARCH ARTICLE

(Department of Surgery, The University of Western Ontario and Department of Biochemistry, The University of Western Ontario) for assistant with the cell culture study. We are particularly grateful for technical support given by Karen Nygard and Dr. Richard Gardiner (Biotron Experimental Climate Change Research Center University of Western Ontario) with the SEM, TEM and confocal microscopy work. We would also like to thank the Western Nanofabrication Facility, the Western Physics and Astronomy Machine Shop and the University Machine Services Shop at the University of Western Ontario for their assistance. This work was supported by a grant from the Ontario Research Fund—Research Excellence program and Axcelon Biopolymers Corp.

References and Notes

1. D. Li, J. T. McCann, Y. Xia, and M. Marquez, Electrospinning: A simple and versatile technique for producing ceramic nanofibers and nanotubes. *J. Am. Ceram. Soc.* 89, 1861 **(2006)**.
2. N. Bhardwaj and S. C. Kundu, Electrospinning: A fascinating fiber fabrication technique. *Biotechnol. Adv.* 28, 325 **(2010)**.
3. S. Chakraborty, I. Liao, A. Adler, and K. W. Leong, Electrohydrodynamics? A facile technique to fabricate drug delivery systems. *Adv. Drug Deliv. Rev.* 61, 1043 **(2009)**.
4. H. S. Yoo, T. G. Kim, and T. G. Park, Surface-functionalized electrospun nanofibers for tissue engineering and drug delivery. *Adv. Drug Deliv. Rev.* 61, 1033 **(2009)**.
5. J. Zeng, X. Xu, X. Chen, Q. Liang, X. Bian, L. Yang, and X. Jing, Biodegradable electrospun fibers for drug delivery. *J. Control. Release* 92, 227 **(2003)**.
6. D. Liang, B. S. Hsiao, and B. Chu, Functional electrospun nanofibrous scaffolds for biomedical applications. *Adv. Drug Deliv. Rev.* 59, 1392 **(2007)**.
7. T. J. Sill and H. A. von Recum, Electrospinning: Applications in drug delivery and tissue engineering. *Biomaterials* 29, 1989 **(2008)**.
8. B. Ding, M. Wang, J. Yu, and G. Sun, Gas sensors based on electrospun nanofibers. *Sensors* (*Basel*) 9, 1609 **(2009)**.
9. X.-H. Qin and S.-Y. Wang, Filtration properties of electrospinning nanofibers. *J. Appl. Polym. Sci.* 102, 1285 **(2006)**.
10. R. Gopal, S. Kaur, Z. Ma, C. Chan, S. Ramakrishna, and T. Matsuura, Electrospun nanofibrous filtration membrane. *J. Memb. Sci.* 281, 581 **(2006)**.
11. R. Barhate and S. Ramakrishna, Nanofibrous filtering media: Filtration problems and solutions from tiny materials. *J. Memb. Sci.* 296, 1 **(2007)**.
12. K. M. Yun, C. J. Hogan, Y. Matsubayashi, M. Kawabe, F. Iskandar, and K. Okuyama, Nanoparticle filtration by electrospun polymer fibers. *Chem. Eng. Sci.* 62, 4751 **(2007)**.
13. A. Frenot and I. S. Chronakis, Polymer nanofibers assembled by electrospinning. *Curr. Opin. Colloid Interface Sci.* 8, 64 **(2003)**.
14. H. Pan, L. Li, L. Hu, and X. Cui, Continuous aligned polymer fibers produced by a modified electrospinning method. *Polymer* 47, 4901 **(2006)**.
15. L. M. Bellan and H. G. Craighead, Control of an electrospinning jet using electric focusing and jet-steering fields. *J. Vac. Sci. Technol. B* 24, 3179 **(2006)**.
16. Z. M. Huang, Y. Z. Zhang, M. Kotaki, and S. Ramakrishna, A review on polymer nanofibers by electrospinning and their applications in nanocomposites. *Compos. Sci. Technol.* 63, 2223 **(2003)**.
17. S. A. Theron, E. Zussman, and A. L. Yarin, Experimental investigation of the governing parameters in the electrospinning of polymer solutions. *Polymer* 45, 2017 **(2004)**.
18. T. A. Kowalewski and S. Barral, Experiments and modelling of electrospinning process. *Bull. Pol. Ac.: Tech.* 53, 385 **(2005)**.
19. D. H. Reneker and A. L. Yarin, Electrospinning jets and polymer nanofibers. *Polymer* 49, 2387 **(2008)**.
20. D. H. Reneker, A. L. Yarin, H. Fong, and S. Koombhongse, Bending instability of electrically charged liquid jets of polymer solutions in electrospinning. *J. Appl. Phys.* 87, 4531 **(2000)**.
21. C. J. Thompson, G. G. Chase, A. L. Yarin, and D. H. Reneker, Effects of parameters on nanofiber diameter determined from electrospinning model. *Polymer* 48, 6913 **(2007)**.
22. S. Saehana, F. Iskandar, and M. Abdullah, Optimization of electrospinning parameter by employing genetic algorithm in order to produce desired nanofiber diameter. *Int. J. Chem. Nucl. Metall. Mater. Eng.* 1, 78 **(2013)**.
23. C. Wang, K.-W. Yan, Y.-D. Lin, and P. C. H. Hsieh, Biodegradable core/shell fibers by coaxial electrospinning: Processing, fiber characterization, and its application in sustained drug release. *Macromolecules* 43, 6389 **(2010)**.
24. A. K. Moghe and B. S. Gupta, Coaxial electrospinning for nanofiber structures: Preparation and applications. *Polym. Rev.* 48, 353 **(2008)**.
25. Z. Sun, E. Zussman, A. L. Yarin, J. H. Wendorff, and A. Greiner, Compound core–shell polymer nanofibers by co-electrospinning. *Adv. Mater.* 15, 1929 **(2003)**.
26. L. Viry, S. E. Moulton, T. Romeo, C. Suhr, D. Mawad, M. Cook, and G. G. Wallace, Emulsion-coaxial electrospinning: Designing novel architectures for sustained release of highly soluble low molecular weight drugs. *J. Mater. Chem.* 22, 11347 **(2012)**.
27. T. T. T. Nguyen, O. H. Chung, and J. S. Park, Coaxial electrospun poly(lactic acid)/chitosan (core/shell) composite nanofibers and their antibacterial activity. *Carbohydr. Polym.* 86, 1799 **(2011)**.
28. C. Yang, Z. Jia, Z. Xu, K. Wang, Z. Guan, and L. Wang, Comparisons of fibers properties between vertical and horizontal type electrospinning systems, *Proceedings of the 2009 IEEE Electrical Insulation and Dielectric Phenomena*, Virginia Beach, VA, October **(2009)**, pp. 18–21.
29. D. Rodoplu and M. Mutlu, Effects of electrospinning setup and process parameters on nanofiber morphology intended for the modification of quartz crystal microbalance surfaces. *J. Eng. Fiber. Fabr.* 7, 118 **(2012)**.
30. L. Vi, A. Njarlangattil, Y. Wu, B. S. Gan, and D. B. O'Gorman, Type-1 collagen differentially alters beta-catenin accumulation in primary dupuytren's disease cord and adjacent palmar fascia cells. *BMC Musculoskelet. Disord.* 10, 72 **(2009)**.
31. M. Mekhail, K. K. H. Wong, D. T. Padavan, Y. Wu, D. B. O'Gorman, and W. Wan, Genipin-cross-linked electrospun collagen fibers. *J. Biomater. Sci. Polym. Ed.* 22, 2241 **(2011)**.
32. V. Beachley and X. Wen, Effect of electrospinning parameters on the nanofiber diameter and length. *Mater. Sci. Eng. C. Mater. Biol. Appl.* 29, 663 **(2009)**.
33. I. Marginean, P. Nemes, and A. Vertes, Order-chaos-order transitions in electrosprays: The electrified dripping faucet. *Phys. Rev. Lett.* 97, 064502 **(2006)**.
34. X. Chen, L. Jia, X. Yin, J. Cheng, and J. Lu, Spraying modes in coaxial jet electrospray with outer driving liquid. *Phys. Fluids* 17, 032101 **(2005)**.
35. E. Lee, Core–shell nanofibres for heart valve leaflet tissue engineering [dissertation]. London (ON, Canada), The University of Western Ontario **(2011)**.
36. I. C. Liao, S. Y. Chew, and K. W. Leong, Aligned core–shell nanofibers delivering bioactive proteins. *Nanomedicine* 1, 465 **(2006)**.
37. R. M. Nezarati, M. B. Eifert, and E. Cosgriff-Hernandez, Effects of humidity and solution viscosity on electrospun fiber morphology. *Tissue Eng. Part C. Methods* 19, 810 **(2013)**.

Delivered by Publishing Technology to: Xinyu Li
IP: 129.100.226.75 On: Tue, 24 Nov 2015 19:56:22
Copyright: American Scientific Publishers

Received: 4 September 2014. Revised/Accepted: 15 October 2014.

RESEARCH ARTICLE